
Climate Data Record (CDR) Program

Climate Algorithm Theoretical Basis Document (C-ATBD)

Outgoing Longwave Radiation (OLR) - Daily



CDR Program Document Number: CDRP-ATBD-0526

Configuration Item Number: 01B-21

Revision 1 / June 1, 2014

DSR Number: DSR-661

TABLE of CONTENTS

1. INTRODUCTION.....	7
1.1 Purpose.....	7
1.2 Definitions.....	7
1.3 Document Maintenance.....	Error! Bookmark not defined.
2. OBSERVING SYSTEMS OVERVIEW.....	8
2.1 Products Generated	9
2.2 Instrument Characteristics	9
3. ALGORITHM DESCRIPTION.....	13
3.1 Algorithm Overview	13
3.2 Processing Outline.....	13
3.3 Algorithm Input.....	15
3.3.1 Primary Sensor Data	15
3.3.2 Ancillary Data.....	16
3.3.3 Derived Data	17
3.3.4 Forward Models.....	18
3.4 Theoretical Description	18
3.4.1 Physical and Mathematical Description.....	19
3.4.2 Data Merging Strategy.....	20
3.4.3 Numerical Strategy	23
3.4.4 Calculations.....	24
3.4.5 Look-Up Table Description.....	25
3.4.6 Parameterization	25
3.4.7 Algorithm Output.....	26
4. TEST DATASETS AND OUTPUTS.....	27
4.1 Test Input Datasets	27
4.2 Test Output Analysis	27
4.2.1 Reproducibility.....	27
4.2.2 Precision and Accuracy	27
4.2.3 Error Budget.....	31
5. PRACTICAL CONSIDERATIONS.....	32
5.1 Numerical Computation Considerations.....	32
5.2 Programming and Procedural Considerations	32
5.3 Quality Assessment and Diagnostics	32
5.4 Exception Handling	32
5.5 Algorithm Validation	33
5.6 Processing Environment and Resources	34
6. ASSUMPTIONS AND LIMITATIONS	35

6.1 Algorithm Performance 35

6.2 Sensor Performance 36

7. FUTURE ENHANCEMENTS..... 37

7.1 Enhancement 1 – Missing Daily Fields 37

7.2 Enhancement 2 – Gridsat Quality Control 37

7.3 Enhancement 3 – Temporal Integral Scheme 37

7.4 Enhancement 4 – Hyperspectral OLR Algorithms..... 37

8. REFERENCES..... 39

APPENDIX A. ACRONYMS AND ABBREVIATIONS..... 41

APPENDIX B. GRIDSAT OLR RETRIEVAL ALGORITHM 43

APPENDIX C. GSIP OLR RETRIEVAL ALGORITHM..... 45

LIST of FIGURES

Figure 1 DAILY OLR CDR production system overview.	14
Figure 2 DAILY OLR CDR production flow chart.	15
Figure 3 TOA upward longwave radiation spectrum for standard mid-latitude summer case. The smooth curves are the Planck function evaluated at 200°K, 250°K and 294°K (surface temperature for this case), respectively for reference purpose.....	19
Figure 4 Example 7-day boxcar for day 180 of year 1995 on the grid cell [207,98]. The Imager OLR (black stars) is calibrated against the HIRS OLR (red points). The calibrated Imager OLR (blue diamonds) is obtained through the linear function determined by the regression on the coincident HIRS/Imager OLR pairs. The daily OLR for the target day (between the two green lines) is derived with trapezoidal rule applying to all OLR data, including the HIRS OLR and the calibrated Imager OLR data. To visualize the temporal integration, the red curve indicates the OLR variation described with combined HIRS and Imager OLR, after the Imager OLR is linear adjusted. The blue curve represents that when the imager OLR is adjusted only by the Offset, while the cyan curve represents that when the Imager OLR is adjusted by the scaling method (which is not used in this algorithm). The impact of the Imager OLR calibration can be seen as the gap between the black curve (connecting the original Imager OLR data points) and the red curve, with the latter represents the “best estimate” of the OLR diurnal variations with the blended information.....	23
Figure 5 The OLR differences between Daily OLR CDR v01R02beta3c and the CERES EBAF Ed2.6r on the monthly basis: (a) mean OLR differences, and (b) standard deviation of the OLR differences, over the period of March 2000 to June 2012. Most areas in (a) are shown to have relative biases to within $\pm 3 \text{ Wm}^{-2}$. The purple and blue areas in (b) indicating standard deviations within 0-3 and 3-6 Wm^{-2} , respectively.	28
Figure 6 The time series of the global average of OLR differences between Daily OLR CDR v01R02beta3c and the CERES EBAF Ed2.6r on the monthly basis: mean OLR differences (red curve) and the standard deviation of the OLR differences (purple curve), over the period of March 2000 to June 2012.	28
Figure 7 Comparison of monthly OLR anomalies between the Daily OLR CDR (blue) and the CERES EBAF OLR product (red) over the (a) global and (b) tropical 20S-20N domains. The green curves are for their differences.	29
Figure 8 Comparison of monthly OLR anomalies between the Daily OLR CDR (blue) and the ERBS WFOV OLR product (red) over the tropical 20S-20N domains for 1985-1999 period.	30
Figure 9 Comparison of daily OLR between the Daily OLR CDR (blue) and the CERES SYN1deg OLR product (red) over the (a) global and (b) tropical 20S-20N domains for the March 2000 to Dec 2012 period. The green curves are for their differences.....	30

Figure 10 Time series of the global mean (a) and standard deviation (b) of the daily OLR differences between the Daily OLR CDR and the CERES SYN1deg OLR product. The red points showing larger standard deviation values are for the first day of each month. It is likely that they were caused by processing bugs in the CERES SYN1deg production system. 31

LIST of TABLES

Table 1 Version tracking for the DAILY OLR CDR product releases.	Error! Bookmark not defined.
Table 2 Description of instrument parameters for variant versions of HIRS instruments with an assumed satellite altitude of 833 km.	9
Table 3 Description of HIRS channel spectral locations and sensing properties. The channels that are used by OLR algorithm are shown. Note that the OLR retrieving channels for HIRS/3 and 4 are different from those of HIRS/2.	10
Table 4 Description of HIRS instrument type and Level-1b data set coverage available for the DAILY OLR CDR production.	11
Table 5 HIRS OLR v2.7 intersatellite bias adjustments, in unit Wm^{-2}	17
Table 6 Error sources and best estimated magnitude for HIRS OLR CDR production.	31
Table 7 Coefficients for the One-Channel OLR model.	43
Table 8 Coefficients for the Two-Channel OLR model.	44

1. Introduction

1.1 Purpose

The purpose of this document is to describe the algorithm submitted to the National Climatic Data Center (NCDC) by Dr. Hai-Tien Lee / University of Maryland that will be used to create the Daily Outgoing Longwave Radiation Climate Data Record (CDR), using the radiance observations from the High Resolution Infrared Radiation Sounder (HIRS) instruments on board NOAA TIROS-N series and Eumetsat MetOp polar orbiting satellites, and the Imager instruments on board the operational geostationary satellites. The actual algorithm is defined by the computer program (code) that accompanies this document, and thus the intent here is to provide a guide to understanding that algorithm, from both a scientific perspective and in order to assist a software engineer or end-user performing an evaluation of the code.

1.2 Definitions

Following is a summary of the symbols used to define the algorithm.

Spectral and directional parameters:

$$\mu m = \text{wavelength (micrometer)} \quad (1)$$

$$\nu = \text{wavenumber (cm}^{-1}\text{)} \quad (2)$$

$$\theta = \text{view zenith angle or local zenith angle (degree)} \quad (3)$$

$$\phi = \text{relative azimuth angle (degree)} \quad (4)$$

$$I_{\nu}^{\uparrow}(z, \theta, \phi) = \text{upward specific intensity at height } z \text{ (Wm}^{-2} \text{sr}^{-1} \text{(cm}^{-1}\text{)}^{-1}\text{)} \quad (5)$$

$$\Phi_i(\nu) = \text{normalized spectral response function for the } i^{\text{th}} \text{ channel (unit-less)} \quad (6)$$

$$N_i(\theta, \phi) = \text{TOA radiance observed from satellite for the } i^{\text{th}} \text{ channel (Wm}^{-2} \text{sr}^{-1} \text{(cm}^{-1}\text{)}^{-1}\text{)} \quad (7)$$

$$N_{\Delta\nu}(\theta, \phi) = \text{TOA radiance integrated over wavenumber interval } \Delta\nu \text{ (Wm}^{-2} \text{sr}^{-1}\text{)} \quad (8)$$

$$F^{\uparrow}(z, \theta, \phi) = \text{upward radiant flux intensity at height } z \text{ (Wm}^{-2} \text{sr}^{-1}\text{)} \quad (9)$$

$$F_{\nu}^{\uparrow}(z) = \text{upward spectral flux at height } z \text{ (Wm}^{-2} \text{(cm}^{-1}\text{)}^{-1}\text{)} \quad (10)$$

$$F^{\uparrow}(z) = \text{upward flux (cf. radiant flux density, or irradiance) at height } z \text{ (Wm}^{-2}\text{)} \quad (11)$$

$$B_{\nu}(T) = \text{Planck function evaluated at wavenumber } \nu \text{ at a temperature } T \text{ (Wm}^{-2} \text{sr}^{-1} \text{(cm}^{-1}\text{)}^{-1}\text{)} \quad (12)$$

$$C_1 = \text{First Planck function coefficient } (Wm^{-2} sr^{-1} (cm^{-1})^{-1} (cm^{-1})^{-3}) \quad (13)$$

$$C_2 = \text{Second Planck function coefficient } ((cm^{-1})^{-1} \text{ Kelvin}) \quad (14)$$

Atmospheric parameters:

$$\tau_{\nu}(z, \theta) = \text{optical depth (unit-less)} \quad (15)$$

1.3 Referencing this Document

This document should be referenced as follows:

Outgoing Longwave Radiation - Daily - Climate Algorithm Theoretical Basis Document, NOAA Climate Data Record Program CDRP-ATBD-0526 by CDRP Document Manager Rev. 1 (2014). Available at <http://www.ncdc.noaa.gov/cdr/operationalcdrs.html>

1.4 Document Maintenance

Table 1 describes the versions of the Daily OLR CDR product releases with their corresponding software package and the CATBD versions.

Table 1 Version tracking for the DAILY OLR CDR product releases.

Product Version	Software Version	CATBD Revision	Release Date	Remarks
v01r02	v01r02	1.	2014-06-10	Initial Release

2. Observing Systems Overview

2.1 Products Generated

The product generated is the daily mean OLR time series in 1°x1° equal-angle gridded global maps. For the initial release it spans from January 1st 1979 to the Dec 31st 2012. The data period will be extended to the present day and onwards operationally in the next update release. The OLR is primarily estimated from the HIRS radiance observations for all sky conditions. The HIRS instruments are flown on board the NOAA TIROS-N series and Eumetsat MetOp-A/B operational polar-orbiting satellites. The OLR estimated from Imagers radiance observations on board operational geostationary satellites is incorporated to achieve accurate temporal integration for the daily mean OLR.

OLR is one of the three components that determine the TOA earth radiation budget. OLR has been extensively used in the investigations of the cloud/water vapor/radiative interaction processes, climate variability, and for climate change monitoring and numerical model evaluation and diagnostics, etc. It has also been used to estimate large-scale precipitation. OLR is identified as one of the “Essential Climate Variables” in WMO Global Climate Observing System (GCOS).

2.2 Instrument Characteristics

HIRS is one of the three sounding instruments that constitute the TIROS Operational Vertical Sounder (TOVS, and later becomes Advanced TOVS, ATOVS) system on board the NOAA TIROS-N series and Eumetsat MetOp-A/B satellites. The detailed description of HIRS instrument characteristics, Level-1b data format, the TOVS system, and the system configurations for the NOAA TIROS-N series polar orbiters can be found in the NOAA Polar Orbiter Data (POD) User's Guide (1998 version) and NOAA KLM User's Guide (2009 version).

There are some relatively minor variations in HIRS instrument design. **Table 2** lists the HIRS instrument parameters for the variant versions (cf. NOAA POD User's Guide Table 4.0-1; NOAA KLM User's Guide Section 3.2.2 and Appendix J). It's noteworthy to point out that the on-board warm target calibration reference has been changed from two blackbodies in HIRS/2 and 2I to one blackbody in HIRS/3 and 4. The HIRS/4 FOV resolution is enhanced to 10 km, which is about twice better than the earlier HIRS versions.

Table 2 Description of instrument parameters for variant versions of HIRS instruments with an assumed satellite altitude of 833 km.

Parameters	HIRS/2	HIRS/2I	HIRS/3	HIRS/4
Calibration	Two Stable blackbodies and space	Two Stable blackbodies and space	One Stable blackbody (290K) and space	One Stable blackbody (286K) and space

	background	background	background	background
Cross-track scan angle (degrees from nadir)	± 49.5	± 49.5	± 49.5	± 49.5
Scan time (seconds)	6.4	6.4	6.4	6.4
Number of steps	56	56	56	56
Angular FOV (degrees)	1.22	1.40	1.40 (Ch1-12) 1.3 (Ch13-19)	0.69
Step angle (degrees)	1.8	1.8	1.8	1.8
Step time (seconds)	0.1	0.1	0.1	0.1
Ground IFOV at nadir (km diameter)	17.4	20.4	20.3 (Ch1-12) 18.9 (Ch13-19)	10
Ground IFOV at end of scan	58.5 km cross-track x 29.9 km along-track	68.3 km cross-track x 34.8 km along-track	68.3 km cross-track x 34.8 km along-track	34.2 km cross-track x 17.4 km along-track
Distance between IFOV centers (km along-track)	42.0	42.0	42	42
Swath width	± 1120 km	± 1124 km	± 1124 km	± 1107 km
Data precision (bits)	13	13	13	13

HIRS consists of nineteen infrared channels (channels 1-19) and one visible channel (channel 20). **Table 3** lists the central wavenumbers and the sensing properties for the HIRS/2 on NOAA-9 as an example, with the channels used in HIRS OLR algorithm indicated. Specifications for HIRS/3 and 4 are available on NOAA KLM User's Guide.

Table 3 Description of HIRS channel spectral locations and sensing properties. The channels that are used by OLR algorithm are shown. Note that the OLR retrieving channels for HIRS/3 and 4 are different from those of HIRS/2.

Channel	Central wavenumber (cm ⁻¹)	Used in HIRS/2 OLR Algorithm	Sensing Properties
1	667.67		15 μm CO ₂ band
2	679.84		15 μm CO ₂ band
3	691.46	✓	15 μm CO ₂ band

4	703.37		15 μm CO ₂ band
5	717.16		15 μm CO ₂ band
6	732.64		15 μm CO ₂ band
7	749.48	✓	15 μm CO ₂ band
8	898.53	✓	Window
9	1031.61		Ozone
10	1224.74		Water Vapor
11	1365.12	✓	Water Vapor
12	1483.24	✓	Water Vapor
13	2189.97		4.3 μm CO ₂ band
14	2209.18		4.3 μm CO ₂ band
15	2243.14		4.3 μm CO ₂ band
16	2276.46		4.3 μm CO ₂ band
17	2359.05		4.3 μm CO ₂ band
18	2518.14		Window
19	2667.80		Window
20	14549.27		Visible Window

Table 4 describes the HIRS instrument types and the availability of HIRS Level-1B data. The near real-time instrument health condition is available at NESDIS POES Status Monitoring website (<http://www.oso.noaa.gov/poesstatus/> as of May 1, 2014). The satellite ID is the code name for these polar orbiters that will be referred in the DAILY OLR CDR production package and in this document henceforth.

Errata: The Note 7 of Table J.1 on KLM User's Guide Appendix J states that "HIRS/2I was flown on NOAA-14 only". This statement is incorrect. HIRS/2I instruments were flown on both NOAA-11 and 14.

Table 4 Description of HIRS instrument type and Level-1b data set coverage available for the DAILY OLR CDR production.

Satellite	Satellite ID	Data coverage	Instrument Type
TIROS-N (TN)	N05	1978 d294 – 1980 d054	HIRS/2
NOAA-6 (NA)	N06	1979 d181 – 1983 d064 1985 d098 – 1985 d181 1985 d290 – 1986 d319	HIRS/2
NOAA-7 (NC)	N07	1981 d236 – 1985 d032	HIRS/2

NOAA-8	(NE)	N08	1983 d123 – 1984 d163 1985 d182 – 1985 d287	HIRS/2
NOAA-9	(NF)	N09	1984 d348 – 1988 d312	HIRS/2
NOAA-10	(NG)	N10	1986 d329 – 1991 d259	HIRS/2
NOAA-11	(NH)	N11	1988 d313 – 1995 d100 1997 d196 – 2000 d117	HIRS/2I
NOAA-12	(ND)	N12	1991 d259 – 1998 d348	HIRS/2
NOAA-14	(NJ)	N14	1995 d001 – 2006 d283	HIRS/2I
NOAA-15	(NK)	N15	1998 d299 – 2009 d120	HIRS/3
NOAA-16	(NL)	N16	2001 d001 – present	HIRS/3
NOAA-17	(NM)	N17	2002 d191 – 2013 d099	HIRS/3
NOAA-18	(NN)	N18	2005 d156 – present	HIRS/4
NOAA-19	(NP)	N19	2009 d153 – present	HIRS/4
MetOp-A	(M2)	N20	2006 d325 – present	HIRS/4
MetOp-B	(M1)	N21	2013 d015 – present	HIRS/4

3. Algorithm Description

3.1 Algorithm Overview

The multi-spectral OLR estimation method was developed by Ellingson et al. (1989) that use narrowband radiance observations from the High-resolution Infrared Sounder (HIRS) to estimate TOA total longwave flux. Vigorous validation efforts were performed for the HIRS OLR estimation technique against broadband observations derived from the Earth Radiation Budget Experiment (ERBE) and the Clouds and the Earth's Radiant Energy System (CERES) (see Ellingson et al., 1994; Lee et al., 2007). The multi-spectral OLR estimation technique has been adapted successfully to the GOES- Sounder (Ba et al., 2003) and GOES-Imager instruments (Lee et al., 2004). These studies have shown that this OLR estimation algorithm can reliably achieve with an accuracy of about 4 to 8 Wm^{-2} for various instrument type, with biases (precision) that are within the respective radiometric accuracy of the reference instruments. The HIRS OLR algorithm has been implemented to generate the NESDIS operational HIRS OLR product since September 1998, and the GOES Imager OLR is implemented as part of the operational GOES Surface and Insolation Product (GSIP). A variant of this method has been developed and implemented for the upcoming GOES-R Advanced Baseline Imager instrument (Lee et al., 2010).

3.2 Processing Outline

The Daily OLR CDR algorithm main components include the HIRS radiance calibration, OLR retrievals (HIRS and Imagers), the HIRS/Imager OLR blending procedure, and the temporal integration that determines the daily mean OLR at each $1^{\circ} \times 1^{\circ}$ grid box.

The diurnal variation information is resolved with the geostationary satellite observations. The Gridsat CDR product (Knapp et al., 2011) provides the inter-calibrated and limb-corrected brightness temperatures for window and water vapor channels. The Gridsat OLR is estimated with an algorithm adapted from the AVHRR OLR algorithm (Ohring et al., 1984) and is calibrated against the HIRS OLR retrievals to maintain absolute radiometric accuracy.

The HIRS/Imager OLR blending procedure performs the inter-calibration of the HIRS and Imager OLR, the temporal interpolation for missing (e.g., for orbital gaps over the tropics), and the daily integral. This is carried out over a “7-day boxcar” for each of the $1^{\circ} \times 1^{\circ}$ grid boxes, where the “7-day boxcar” is a moving boxcar unit spanning 7 days centered on the target day.

For Interim Daily OLR CDR production, the NESDIS operational Geostationary Surface Insolation Product (GSIP) OLR product is used that replaces the Gridsat OLR. The GSIP OLR is determined from multi-spectral OLR algorithm, similar to the HIRS OLR, with the Imager radiance observations.

Figure 1 provides the overview for the Daily OLR CDR production system. **Figure 2** is the Daily OLR CDR production flow chart that explains the execution sequences and input/output relationships.

HIRS Daily OLR CDR Production System Overview

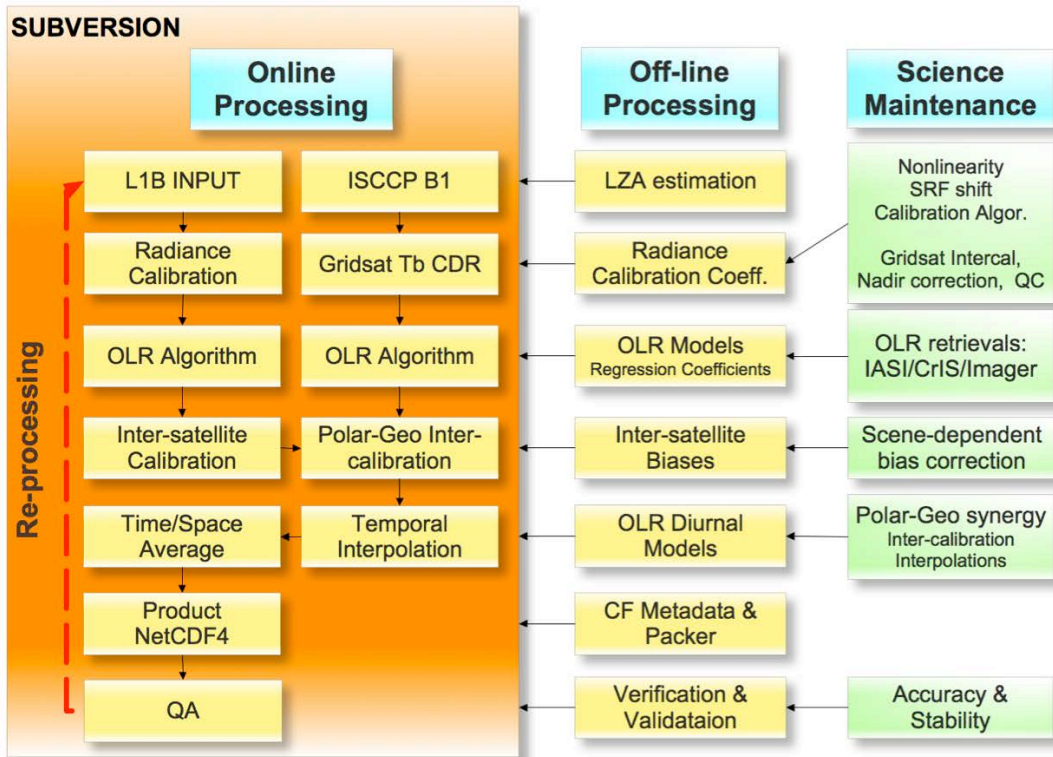
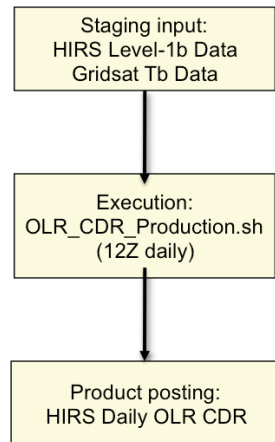


Figure 1 DAILY OLR CDR production system overview.

HIRS OLR CDR Production Flow Chart

Operational Daily Execution



Top View Flow Chart

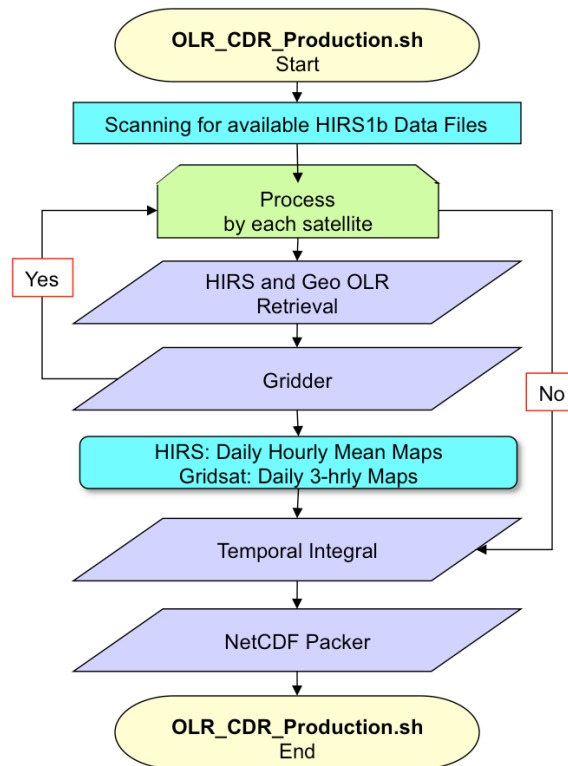


Figure 2 DAILY OLR CDR production flow chart.

3.3 Algorithm Input

3.3.1 Primary Sensor Data

For final CDR production, the dynamic input data for the Daily OLR CDR algorithm include the radiance data from HIRS and Imager instruments. The HIRS Level-1B data, available from NCDC CLASS, is used to determine the HIRS radiances. The Gridsat CDR product (CDR Program) provides the Imager brightness temperatures.

For interim CDR production, the GSIP OLR substitutes the Gridsat-based Imager OLR. The GSIP product is available on the NCDC CLASS system.

3.3.2 Ancillary Data

There are three groups of ancillary data (namely, the static data) that are required for the Daily OLR CDR production: a) the OLR regression coefficients, b) the calibration prediction coefficients; c) OLR inter-satellite bias adjustments. These static data are satellite-specific.

a. OLR Regression Coefficients

The coefficients for the OLR regression model are derived from a set of 3200 simulated fluxes and radiances (see Ellingson et al. 1989 and Lee et al. 2007 for details). The version of the OLR regression coefficients is defined by the version of radiative transfer model simulations. The regression coefficients included in this package were generated according to Lee (2014), with a version code name “v2.7”.

Format	ASCII tabulated, 5 columns x 6501 lines
Version	V2.7 (M2S3/Phillips Soundings)
Size	430K B each; Total 6.5 MB for 15 files (N05-N21).
Location	/Data_static/OLR_coef/coef_{\$satid}_305_a19.asc (refer /Scripts/OLR_retrieval.sh)
Access	Local
Reference	Lee, H.-T., 2014 “Daily OLR CDR – Development and Evaluation”

b. Calibration Prediction Coefficients

There are sets of coefficients that are required by the McMillin radiance calibration method (NOAA POD Users Guide, 1998). They are also satellite specific. The generation and updates of these coefficients are discussed in Lee et al. (2007) and the technical report “McMillin HIRS Radiance Calibration Method”.

Format	ASCII
Version	Ver.1: N05 – N12 Ver.2: N14 Ver.3: N15 – N21 (Refer /Utility/define_pred_version.sh)
Size	25 KB per satellite; Total 375 KB.
Location	/Data_static/cali_data/{\$satid} (refer /Scripts/OLR_retrieval.sh)
Access	Local
Reference	/Documentations/Publications/Lee 2007 HIRS OLR CDR.pdf /Documentations/Tech_Report/McMillin HIRS Radiance Calibration Method.pdf

c. OLR Intersatellite Bias Adjustments

The methodology for deriving the bias adjustments are described in Lee et al. (2007) with the update to reflect the v2.7 OLR retrievals. The Adjustment amount is to be subtracted from the OLR retrievals of the corresponding satellite.

Format	ASCII
Version	V2.7
Size	4 KB
Location	/Data_static/Intersat_Adjustment_Ed2.7.dat (refer /Scripts/OLR_daily_integral.sh)
Access	Local
Reference	Table 5

Table 5 HIRS OLR v2.7 intersatellite bias adjustments, in unit Wm^{-2} .

Satellite ID	Ver.2.7
N05	-0.13
N06	-0.36
N07	-0.28
N08	0.00
N09	0.00
N10	-0.15
N11	-0.53
N12	-0.23
N14	-0.16
N15	0.49
N16	0.50
N17	0.53
N18	-0.03
N19	0.24
N20	0.10
N21	-0.01

3.3.3 Derived Data

Not applicable.

Remark: The radiance calibration module takes the HIRS Level-1B data as the input and derives the HIRS radiance. The radiance is then passed directly to the OLR regression model without being written to an intermediate data file.

3.3.4 Forward Models

Not applicable.

3.4 Theoretical Description

The HIRS CDR OLR production is a sequential processing. The sequence and the relevant processing are described here. See “OLR_CDR_Production.sh” script file for more details.

a. Radiance Calibration

The Daily OLR CDR production starts with the derivation of the radiance from the HIRS Level-1B data by the radiance calibration module. The radiance calibration is performed consistently throughout the HIRS OLR time series with the McMillin radiance calibration method.

b. OLR Retrieval (HIRS and Imager)

The multi-spectral OLR estimation technique is applied here. The HIRS OLR is retrieved at each HIRS FOV with the given radiances and local zenith angles. The Gridsat OLR is retrieved each of the 0.07° Gridsat grid boxes.

c. HIRS OLR Intersatellite Bias Adjustment

Inter-satellite calibration of HIRS OLR retrievals are performed by applying the pre-determined bias adjustments relative to the reference HIRS on NOAA-9 satellite.

d. Gridding of OLR hourly Maps

For each satellite, one month worth of FOV OLR retrievals are compiled and gridded into hourly 1°x1° equal-angle maps using UTC time stamp. The Imager OLR is gridded into 3-hourly 1°x1° maps, time-stamped at the nominal hours, i.e., 00Z, 03Z..etc.

e. HIRS/Imager Inter-calibration and temporal integration

At each 1° grid box in a 7-day boxcar unit (centered on the target day), the coincident Imager OLR and HIRS OLR pairs are used to calibrate the Imager OLR towards the HIRS. Given that the Imager and HIRS OLR have now reached the same absolute radiometric level, the daily integral is performed using trapezoidal rule with all available OLR data, at a nominal interval of 3 hours.

f. NetCDF packing

The Daily OLR CDR NetCDF files are packed annually for both the final and interim CDR products.

3.4.1 Physical and Mathematical Description

The specific intensity I_ν of upward longwave radiation at the top of the atmosphere z_t at local zenith angle θ and azimuth angle ϕ can be expressed as:

$$I_\nu^\uparrow(z_t; \theta, \phi) = \varepsilon_\nu^* B_\nu^*(0) T_\nu^*(z_t, 0; \theta, \phi) + \int_0^{z_t} B_\nu(z') \frac{\partial T_\nu(z_t, z'; \theta, \phi)}{\partial z'} dz' \quad (16)$$

where T_ν is the monochromatic atmospheric transmittance, T_ν denotes the surface emissivity, $B_\nu(z')$ is the Planck function evaluated at wavenumber ν with the temperature at level z' . The black surface is assumed here.

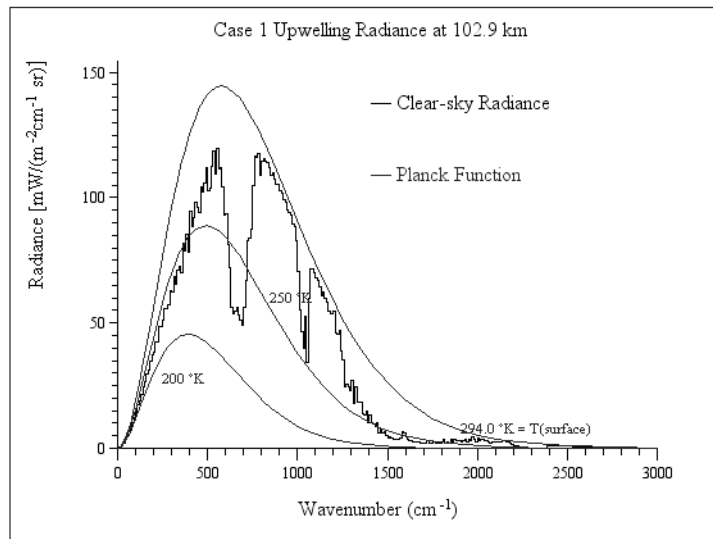


Figure 3 TOA upward longwave radiation spectrum for standard mid-latitude summer case. The smooth curves are the Planck function evaluated at 200°K, 250°K and 294°K (surface temperature for this case), respectively for reference purpose.

The outgoing longwave radiation (*OLR*), whose example spectrum is shown in **Figure 3**, is the radiative flux through a unit area at the top of the atmosphere that is related to the specific intensity by integrating over wavenumbers ν and over hemispheric solid angles (θ and ϕ):

$$OLR = \int_0^{2\pi} \int_0^{\pi/2} \int_0^{\infty} I_\nu^\uparrow(z_t; \theta, \phi) \cos \theta d\nu \sin \theta d\theta d\phi \quad (17)$$

Ellingson et al. (1989) formulated the multi-spectral OLR algorithm that expresses the OLR as a linear combination of the radiances (N_i) of selected channels, observed at a local zenith angle θ :

$$OLR = a_0(\theta) + \sum_i a_i(\theta) \cdot N_i(\theta) \quad (18)$$

where a_0 and a_i are the regression coefficients.

The satellite-observed narrowband radiance N_i of channel i can be described by the convolution of the TOA specific intensity with the respected spectral response function Φ_i

$$N_i(\theta, \phi) = \int_{\nu} \hat{I}_\nu(z_i; \theta, \phi) \cdot \Phi_i(\nu) d\nu \quad (19)$$

The azimuth angle dependence in the radiance is removed when axel-symmetry is assumed. The wavenumber interval is defined as from 0 to 3000 cm^{-1} .

The new v2.7 HIRS OLR algorithm developed for the daily OLR CDR is revised to included non-linear radiance terms in the predictors, generalized in this form:

$$OLR = a_0(\theta) + \sum_i a_i(\theta) \cdot N_i^p(\theta) \quad (20)$$

where p denotes the power that corresponding channel radiance is being raised.

The v2.7 HIRS OLR model now consists of the radiance predictors from HIRS channels: 3, 7, 8, 11, 8², 11^{0.5}, 12^{0.5}, with the exponents indicating the raised powers, such as this:

$$OLR = a_0(\theta) + a_1(\theta) \cdot N_3(\theta) + a_2(\theta) \cdot N_7(\theta) + a_3(\theta) \cdot N_8(\theta) + a_4(\theta) \cdot N_{11}(\theta) \\ + a_5(\theta) \cdot N_8^2(\theta) + a_6(\theta) \cdot N_{11}^{0.5}(\theta) + a_7(\theta) \cdot N_{12}^{0.5}(\theta) \quad (21)$$

The OLR regression coefficients are determined from a set of 3717 radiation simulations by the Warner-Ellingson radiative transfer model (Warner and Ellingson, 2000) with Phillips soundings (termed m2s3 simulation method).

The OLR algorithm for deriving OLR from Gridsast CDR data is described in Appendix B, and the OLR algorithm for GSIP OLR production is described in Appendix C.

3.4.2 Data Merging Strategy

The Daily OLR CDR production uses multi-platforms observations that require critical data merging techniques to achieve consistency and continuity. The critical components are the OLR retrieval and the temporal integral.

a. OLR Retrieval

Obtaining consistent OLR retrievals from all satellites is achieved through two controlling factors: 1) consistent OLR regression models; 2) inter-satellite calibration.

The coefficients for OLR regression models are satellite/instrument specific. Since the coefficients are derived from a common set of simulations, the OLR regression

models for different satellites and instruments would have consistent error characteristics, if the instruments are not changed. However, due to the variations in HIRS/2/2I/3, and 4, there are necessary changes in the OLR regression model formulation, which could result in inconsistencies in their regression error characteristics. This in turn will reduce the robustness of the inter-satellite calibration results. The new v2.7 OLR models use radiance observations available to all versions of HIRS instruments that significantly improved the consistency of OLR retrievals and reduced the residual errors in the inter-satellite calibrations.

The inclusion of extra opaque high cloud (S3 simulation scheme) extends OLR samples in the low-end range. The OLR regression residual behavior is much improved when the non-linear radiance predictor terms were included. The combined effect is the elimination of end-zone biases, particularly at the low-end of OLR values. The consistency in the residual behavior between OLR models and the removal of low-end biases helps to secure the inter-satellite calibration that primarily relies on polar data due to collocation limitations.

b. Temporal Integral

Polar orbiters have low temporal sampling rate – twice a day for a given location from each satellite. The daily OLR can be erred by as much as 100 Wm^{-2} locally if diurnal variation is not accounted for accurately yet the daily diurnal variation is too transient to be described by static diurnal models. The geostationary observations, with a 30-minute to 3-hourly refresh rate over full disk domains, can be used to provide the OLR diurnal variation information needed for accurate daily OLR determination.

The atmospheric window channel is common to the Imager instruments on board all geostationary satellites, while some have a $6.7\mu\text{m}$ water vapor channel. We can estimate OLR from these observations, although with uncertainties about 3 to 4 times larger than those of HIRS OLR retrievals because the Imager observations lack of atmospheric vertical structure information.

A blending procedure is devised to merge HIRS/Imager OLR data for the daily OLR determination. Since the HIRS OLR retrieval has higher precision and is considered as the absolute radiometric reference, the Imager OLR is adjusted towards the HIRS OLR within a processing unit termed “7-day boxcar” on the grid-by-grid basis (see **Figure 4**).

The blending procedure involves the following steps:

1. HIRS OLR is gridded as hourly data time stamped at the middle of the hour; Imager OLR is gridded as 3-hourly data, stamped at the nominal hours, 00Z, 03Z, ...
2. Construct 7-day boxcar data with HIRS and Imager OLR data
3. Apply Inter-calibration for HIRS OLR. Average HIRS OLR if observations occupy on the same hour box.
4. Interpolate (spline) the Imager OLR to hourly bins and construct coincident HIRS/Imager pairs for use in Imager to HIRS calibration.

5. The Imager to HIRS calibration produces two results: (a) linear adjustment function; (b) an offset (ie., forced with slope one)
6. The linear regression may not always yield reliable results, e.g., when the OLR variation is low (leads to poor signal to noise ratio), or when the fitting has relative low confidence. The method (b) will be applied for either one of the following scenarios:
 - a. HIRS OLR variance is too small ($STD < 20 Wm^{-2}$)
 - b. The explained variance by the linear regression is less than 50%
 - c. When the number of calibration pairs is less than 7
7. Imager OLR data is adjusted and now reaching the same absolute radiometric level as in HIRS
8. Combine Imager OLR with HIRS OLR to form a single hourly time series
9. Apply trapezoidal rules over all available data (at a 3-hourly or better sampling rate) to derive the integral for the target day.
 - a. For full CDR production, the target day is the center (4th day) of the 7-day boxcar
 - b. For interim production, the target day will be on the 6th day for a 36-hr lag production

This process effectively removes scene-dependent biases in the Imager OLR retrievals. The 7-day temporal window provides sufficient number of coincident samples for Imager-to-HIRS calibration purpose while keeping the origins of the biases locally both in space and time (e.g., water vapor variation). It also enables the daily mean derivation even when HIRS is not available due to orbital gap or missing orbits on the target day, once the imager OLR data and its calibration information is available. This procedure essentially eliminates the need of spatial orbital gap filling which can cause relatively large errors even with the optimum interpolation method.

The daily temporal integral can then be accurately determined with all the available OLR data, the HIRS and the calibrated Imager OLR, at a 3-hourly or better temporal sampling interval.

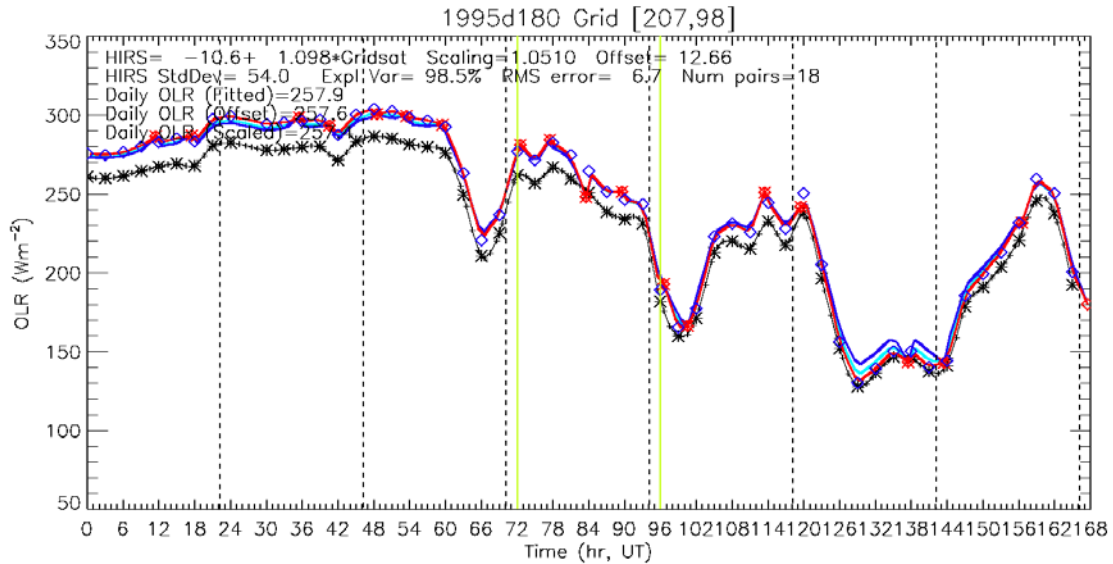


Figure 4 Example 7-day boxcar for day 180 of year 1995 on the grid cell [207,98]. The Imager OLR (black stars) is calibrated against the HIRS OLR (red points). The calibrated Imager OLR (blue diamonds) is obtained through the linear function determined by the regression on the coincident HIRS/Imager OLR pairs. The daily OLR for the target day (between the two green lines) is derived with trapezoidal rule applying to all OLR data, including the HIRS OLR and the calibrated Imager OLR data. To visualize the temporal integration, the red curve indicates the OLR variation described with combined HIRS and Imager OLR, after the Imager OLR is linear adjusted. The blue curve represents that when the imager OLR is adjusted only by the Offset, while the cyan curve represents that when the Imager OLR is adjusted by the scaling method (which is not used in this algorithm). The impact of the Imager OLR calibration can be seen as the gap between the black curve (connecting the original Imager OLR data points) and the red curve, with the latter represents the “best estimate” of the OLR diurnal variations with the blended information.

3.4.3 Numerical Strategy

Missing Value and Weaver Subroutine

The daily mean OLR map could have missing values if the temporal integral performed at certain grid boxes failed, possibly due to insufficient OLR retrieval data. Approximations for such grids will be made with the Cressman interpolation (Cressman, 1959) by the Weaver subroutine.

(Note that for the initial V01R02 release, the bilinear spatial interpolation is employed instead and this will be changed to Weaver method in the next release.)

3.4.4 Calculations

The Daily OLR CDR production involves the following execution components (in sequence):

- a. Compile.sh – Compilation of all Fortran programs used in OLR CDR Production
- b. OLR_CDR_Production.sh - HIRS OLR CDR Production main driver script
 - In automated mode, it is to be executed once a day, presumed to be on the 12Z of the day.
 - It can also be invoked with an argument of <yyyymmdd> to specify the target day to be processed.
- c. OLR_retrieval.sh – HIRS radiance calibration and HIRS OLR retrieval
 - Read HIRS-1b data, perform HIRS radiance calibration for each satellite
 - Calculate HIRS OLR at each HIRS field of view (FOV)
- d. OLR_gridder_v2a.sh and OLR_gridder_v2b.sh–HIRS OLR gridder
 - Grid HIRS FOV OLR retrievals into 1°x1° orbital maps and hourly maps, respectively
- e. Imager_OLR_retrieval_Gridsat.sh – derive Gridsat OLR
 - Read Imager brightness temperatures data from the Gridsat CDR NetCDF data files
 - Calculate Imager OLR at Gridsat native 0.07° grid
 - Grid Imager OLR into 1°x1° 3-hourly maps
 - Note that this is for the Final CDR production
- f. Imager_OLR_retrieval_GSIP.sh – Extract GSIP OLR
 - Extract Imager OLR data from the GSIP NetCDF data files
 - Grid Imager OLR into 1°x1° hourly maps
 - Note that this is for the Interim CDR production
- g. OLR_daily_integral.sh – Intersatellite bias adjustment and daily mean temporal integral
 - Construct 7-day boxcar data array centering on the target day
 - Perform HIRS OLR inter-satellite calibration (static adjustments)
 - Calibrate Imager OLR to HIRS OLR (dynamical adjustments)
 - Perform daily integral to derive daily mean OLR map
- h. OLR_packer_annual.sh – Daily OLR CDR product packing
 - Specify dynamic metadata
 - Pack one year worth of daily OLR fields into one NetCDF-4 data file

3.4.5 Look-Up Table Description

a. Radiance Calibration: Band parameters

Origin	NOAA POD and KLM Users Guide
Construction	4 x 19 per satellite, in ASCII
Usage	Define HIRS channel band central wavenumber and correction coefficients

b. Radiance Calibration: PRT Coefficients

Origin	NOAA POD and KLM Users Guide
Construction	6 x 4 per satellite (N05-N14), in ASCII 5 x 5 per satellite (N15-N17), in ASCII 7 x 5 per satellite (N15-N21), in ASCII
Usage	Define HIRS PRT count to temperature conversion coefficients

c. Radiance Calibration: Temperature prediction coefficients

Origin	Hai-Tien Lee. CICS/UMD
Construction	9 x 19 x 2, in ASCII
Usage	Define temperature prediction coefficients to estimate temperature-dependent calibration coefficients

d. HIRS OLR Regression Coefficients

Origin	Hai-Tien Lee. CICS/UMD
Construction	8 x 6500 in ASCII
Usage	Define OLR regression model

e. Inter-satellite Bias Adjustment

Origin	Hai-Tien Lee. CICS/UMD
Construction	16 x 1 in ASCII
Usage	Define OLR bias adjustments (Wm^{-2})

3.4.6 Parameterization

None.

3.4.7 Algorithm Output

Fully describe the data products produced by the algorithm. This includes generic names and contents, file formats, specific data, physical units, and estimated sizes.

<Enter Text Here>

Name	Daily OLR CDR
Content	Global 1°x1° gridded daily mean OLR time series since January 1 st 1979 to the present
File Format	NetCDF4
Specific Data	hirs_olr_daily_v01r02_197901_19791231.nc (example file name for the annual netCDF data file that contains Daily OLR fields for the year 1979)
Physical Unit	Wm ⁻²
Size	95 MB/Year (OLR field only)

4. Test Datasets and Outputs

4.1 Test Input Datasets

The Daily OLR CDR test data consists of daily OLR time series from 1979 to 2012 using dynamical inputs from all the available HIRS-1b data and the Imager observations extracted from the Gridsat v02r01 CDR product.

4.2 Test Output Analysis

4.2.1 Reproducibility

The software package still partially consists of the developmental IDL codes. The GSIP OLR extraction and interface code for Interim Daily OLR production also awaits to be developed, pending on the release of GSIP v3 updates.

The reproducibility test will be performed when the entire software package is converted to FORTRAN codes and fully automated.

4.2.2 Precision and Accuracy

The precision and accuracy of the Daily OLR CDR product are determined by the comparisons to the reference broadband OLR products. Preliminary evaluations showed very good results. The assessments indicate that the Daily OLR CDR has an accuracy of about 2 Wm^{-2} with a precision of about 2 Wm^{-2} and with a significant improved stability referenced to the CERES EBAF Ed.2.6r, SYN1deg Ed.3A, and ERBS WFOV Non-scanner Ed.3rev1 OLR products (see Lee, 2014a, 2014b).

Figure 5 summarizes the OLR differences between Daily OLR CDR and the CERES EBAF Ed2.6r for about 12 years data record from March 2000 to June 2012, on the monthly basis. The mean and standard deviation of the OLR differences indicate that for the majority of the globe, the Daily OLR CDR is within $\pm 3 \text{ Wm}^{-2}$ relative to the EBAF with standard deviations within 3 Wm^{-2} . Note that the CERES OLR product has an uncertainty of about 1.5%.

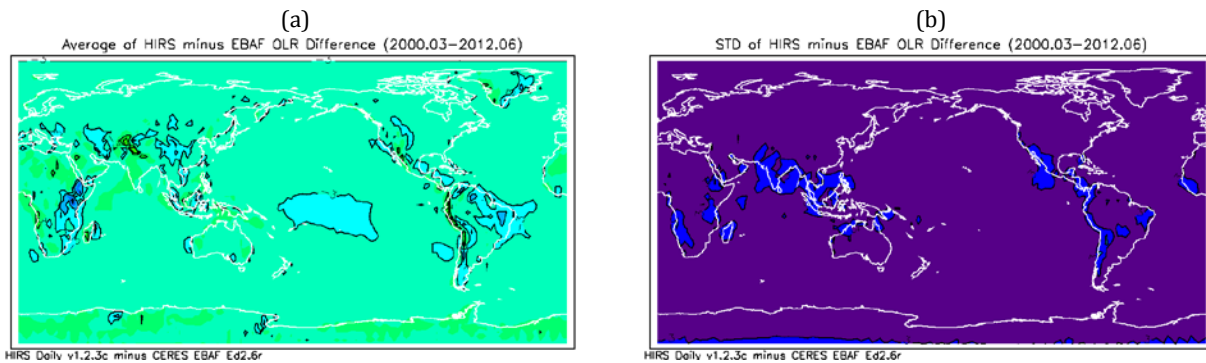


Figure 5 The OLR differences between Daily OLR CDR v01R02beta3c and the CERES EBAF Ed2.6r on the monthly basis: (a) mean OLR differences, and (b) standard deviation of the OLR differences, over the period of March 2000 to June 2012. Most areas in (a) are shown to have relative biases to within $\pm 3 \text{ Wm}^{-2}$. The purple and blue areas in (b) indicating standard deviations within $0-3$ and $3-6 \text{ Wm}^{-2}$, respectively.

The time series of the global average of OLR differences between Daily OLR CDR v01R02beta3c and the CERES EBAF Ed2.6r is shown in **Figure 6**. The global statistics indicate that the Daily OLR CDR has a relative bias of about -2 Wm^{-2} and a precision of about 2 Wm^{-2} relative to the CERES EBAF OLR. The spikes in the standard deviation curve are caused by the missing data in the CERES monthly product where monthly means were derived with only partially observed months.

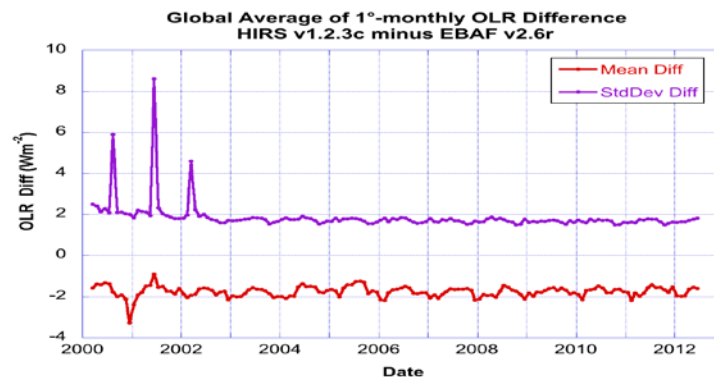


Figure 6 The time series of the global average of OLR differences between Daily OLR CDR v01R02beta3c and the CERES EBAF Ed2.6r on the monthly basis: mean OLR differences (red curve) and the standard deviation of the OLR differences (purple curve), over the period of March 2000 to June 2012.

The comparisons of the monthly OLR anomalies between the Daily OLR CDR and the CERES EBAF OLR product over the global and tropical domains are shown in **Figure 7**. The OLR anomaly variability of the two products tracks each other in excellent synchronization and superb agreement in magnitude. The trends of the OLR anomalies differences for the global and the tropical domains are $0.03 \pm 0.09 \text{ Wm}^{-2}/\text{decade}$ and $0.28 \pm 0.10 \text{ Wm}^{-2}/\text{decade}$, at 2-sigma level, that satisfies the stability requirement for climate quality data: $\pm 0.3 \text{ Wm}^{-2}/\text{decade}$.

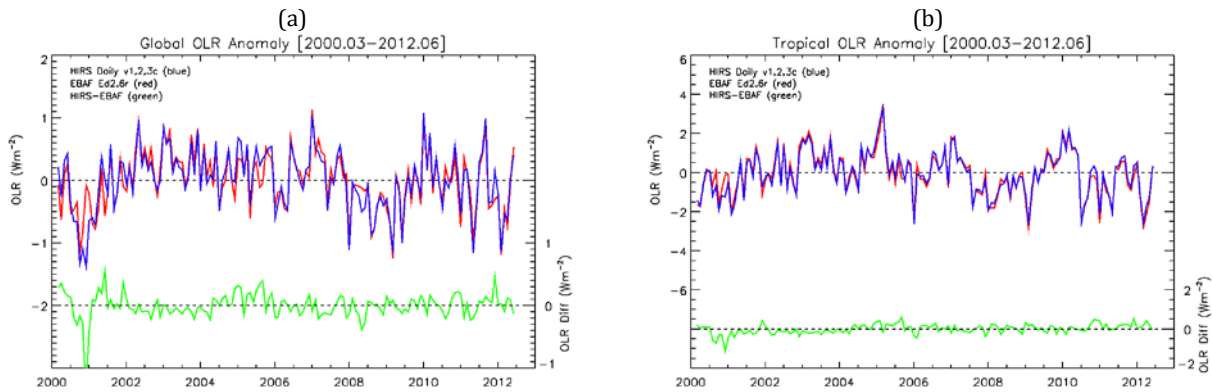


Figure 7 Comparison of monthly OLR anomalies between the Daily OLR CDR (blue) and the CERES EBAF OLR product (red) over the (a) global and (b) tropical 20S-20N domains. The green curves are for their differences.

The comparisons of the monthly OLR anomalies between the Daily OLR CDR and the CERES ERBS OLR product over the tropical domains for the 1985 to 1999 period is shown in **Figure 8**. The differences in spatial and temporal sampling and the temporal integral methods between the two products contribute to the increased diversity compared to the results of HIRS/EBAF comparison. Nevertheless, the two products still show very good agreement in their variability.

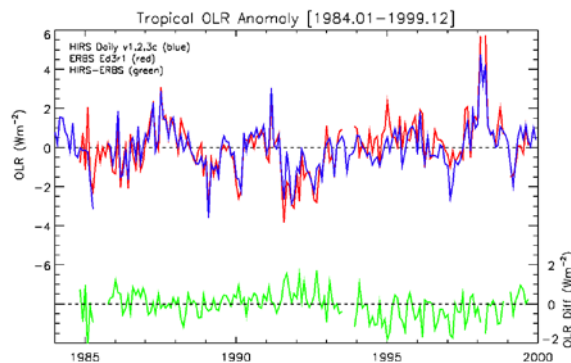


Figure 8 Comparison of monthly OLR anomalies between the Daily OLR CDR (blue) and the ERBS WFOV OLR product (red) over the tropical 20S-20N domains for 1985-1999 period.

The comparisons of the Daily OLR CDR and the CERES SYN1deg OLR product provide assessments on the daily basis. **Figure 9**, similar to Figure 7, but shows the daily OLR anomalies of the two products over the global and the tropical domains. The degrees of the agreement in the OLR anomalies can be easily seen in the difference curves that are comparable to those of the HIRS/EBAF comparisons.

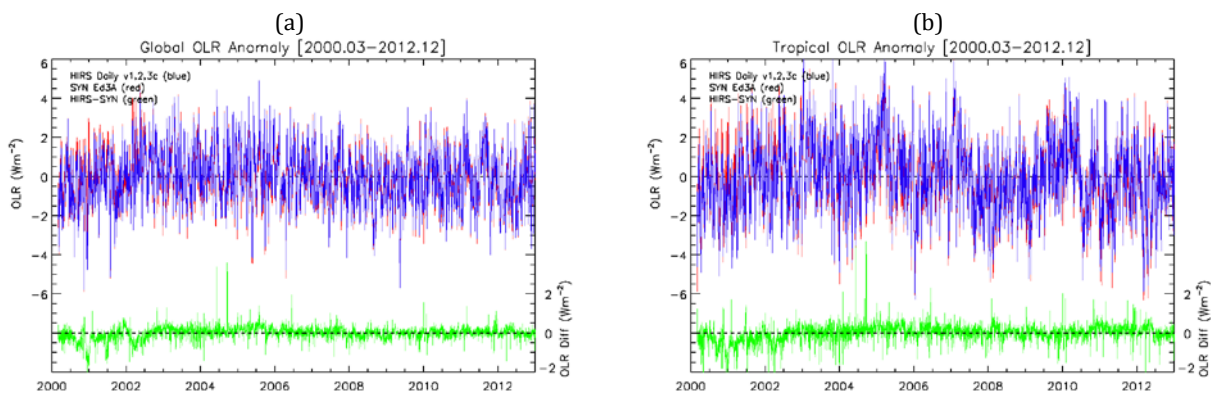


Figure 9 Comparison of daily OLR between the Daily OLR CDR (blue) and the CERES SYN1deg OLR product (red) over the (a) global and (b) tropical 20S-20N domains for the March 2000 to Dec 2012 period. The green curves are for their differences.

The time series of the OLR differences statistics can be used for quality assurance purpose. **Figure 10** shows global mean and standard deviation of the daily OLR differences between the Daily OLR CDR and the CERES SYN1deg OLR product. The slight fluctuation in the global mean OLR differences indicates that there are about 0.5 to 1 Wm⁻² differences in the seasonal cycle between the two products, whereas the Daily OLR CDR is about 1 Wm⁻² lower than the CERES SYN1deg OLR product in average. The overall standard deviation of the OLR differences is about 5 Wm⁻².

Two problems in the CERES SYN1deg OLR product were discovered incidentally. The larger value standard deviations are identified to come from the first day of each month that abnormally large OLR differences were found over the western hemisphere between the Daily OLR CDR and SYN1deg products. This is believed to be caused by processing bugs in the SYN1deg production system. The discontinuity seen in the standard deviation time series indicates the impact of CERES SYN1deg being produced switched from one satellite (Terra only) to two satellites (Terra+Aqua) on mid 2002. This is an

indication that the CERES daily integral scheme, although also employed geostationary observations, may be sensitive to the number or the timing of the polar orbiter observations.

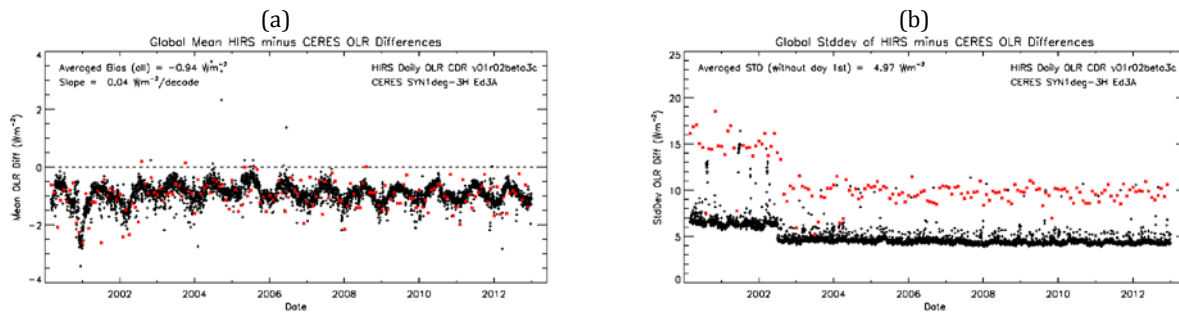


Figure 10 Time series of the global mean (a) and standard deviation (b) of the daily OLR differences between the Daily OLR CDR and the CERES SYN1deg OLR product. The red points showing larger standard deviation values are for the first day of each month. It is likely that they were caused by processing bugs in the CERES SYN1deg production system.

4.2.3 Error Budget

The possible sources of error for Daily OLR CDR derivation are listed in **Table 6**. The best estimates of their magnitude of errors are given. Note that those errors shall not be aggregated in a simple form.

Table 6 Error sources and best estimated magnitude for HIRS OLR CDR production.

Error Sources	Magnitude of Errors	Prospective Improvements
Radiance Calibration	bias at $\sim 0.5^\circ\text{K}$	non-linear calibration method; account for post-launch spectral response function
OLR retrieval	RMS errors ~ 0.5 to 2.5 Wm^{-2}	Scene and angular dependent OLR estimation algorithms; OLR estimation from hyperspectral instruments (Lee et al., 2010)
Intersatellite calibration	biases at ~ 0.5 Wm^{-2}	Scene dependent bias adjustments
Temporal integral	< 5 Wm^{-2} RMS	Using higher temporal resolution of geostationary observations, e.g., SEVIRI, GOES-R

5. Practical Considerations

5.1 Numerical Computation Considerations

a. Endian

The HIRS OLR CDR Production Package assumes IEEE big-endian environment.

b. Precision

The codes can be run under either 32-bit or 64-bit mode.

c. Parallelization

This production package is considered not computationally intensive so that explicit parallelization is not performed.

5.2 Programming and Procedural Considerations

none

5.3 Quality Assessment and Diagnostics

Quality flags fields have been implemented but are not yet included in the netCDF product file.

5.4 Exception Handling

Gridder.f90

The equator crossing time cannot be determined when there are insufficient numbers of near equator observations in a given orbit file. The ECT will be considered missing and is assigned to -1 when that is the case returning to calling routine. The daily mean ECT determination (in grid_OLR.f90) will skip those missing ECT during averaging.

OLR_daily_integral.sh

There were times that quality HIRS observations were not available due to certain temporary malfunction. When this happens over the single POES operation period, the extended missing of HIRS data will result in missing or erroneous daily OLR values. Quality Assurance (QA) check is necessary to identify such days and remove them from data record. Currently there were 205 days that were being identified to be in such scenario and is assigned as completely missing. Most of the missing days occurred during the single satellite operating periods with NOAA-6 and NOAA-9, while most missing day were in the NOAA-9 period. The exact reasons for having poor quality HIRS1b data in those days are not understood. The effectiveness or robustness of such QA check on an operational online system is not assessed yet.

OLR_CDR_nc4_batch.f90

The packing of NetCDF parameters is subject to error check, by subroutine `check_err`. The program will exit if any errors were detected. This will cause failure in the generation of NetCDF product file. This condition will be written to the process log and human interruption will be required.

5.5 Algorithm Validation

Summary

The validation of the Daily OLR CDR algorithm v01r02 has been carried out for the test data spanning from 1979-2012 against the broadband OLR products (Lee 2014a and 2014b). The results are explained in details in Section 4.2.2. The validation assessments have shown that the Daily OLR CDR time series has a stability satisfying the climate quality data requirement, at about 0.3 Wm^{-2} per decade. Globally, Daily OLR CDR agrees with CERES EBAF OLR product within 2 Wm^{-2} with a precision of about 2 Wm^{-2} . This is well within the CERES OLR uncertainty, of about 1.5%.

Validation Strategy

The HIRS OLR retrieval and its daily mean product are evaluated with the radiative flux measurements from broadband instruments, including the ERBS non-scanner, ERBE scanners, and CERES scanners.

For the instantaneous retrieval accuracy assessment, HIRS OLR retrievals at HIRS FOV can be compared against the ERBE/CERES Level-2 single scanner footprint (SSF) product, where the broadband radiance measurement is converted to the total flux at FOV level.

For the evaluation of the daily OLR product, the best validation references currently are the CERES EBAF and SYN1deg OLR products whose daily integral are also performed with the assistance of the geostationary satellite observations. The EBAF product is considered the best earth radiation budget product derived from CERES observations due to its radiometric traceability and the consistency with the ocean heat content measurements. The SYN1deg OLR product, on the other hand, provides the most comparable temporal and spatial resolution for the Daily OLR CDR evaluation purpose.

It is expected to find new releases of the broadband OLR products as well, with improvements in the SRF corrections for the instrument degradation problems. There are also improvements in angular distribution model (ADM) over certain scene types, although globally the impact might be small.

It is necessary to repeat the systematic validations for HIRS OLR CDR with the latest release of the broadband products.

The inter-comparison of the HIRS OLR CDR product with other OLR products and model simulations (e.g., reanalysis products) are beneficiary as well. Multiple sets of inter-comparisons enable us to identify problems in the data sets that are otherwise difficult to affirm, especially when the broadband products are relatively short in time span

and with discontinuities between missions. These exercises can raise the confidence level of the overall validation assessments.

5.6 Processing Environment and Resources

CICS Processing System Configuration

- CPU: MacPro 2x2.4GHz Quad-Core Intel Xeon, 20GB memory
- Operating System: Mac OS X 10.6.8
- Programming Language: Fortran90 and IDL 7.1.1
- Compilers: Intel Fortran v12.1.6
- External Libraries: NetCDF 4.3.0
- Total CPU time (for one day):
- Total Wall clock time (for one day):
- Working space (for 34 years 1979-2012 data): Total about 7TB.
HIRS-1b (2.5 TB), Gridsat (3.2 TB), HIRS Hourly OLR (682GB), Gridsat Hourly OLR (38GB), HIRS daily OLR (3.2GB)

6. Assumptions and Limitations

a. Radiative Transfer Model Simulations

The OLR regression models were constructed with a set of radiative transfer model simulations. As being statistical models, they are assumed to be representative for global application in all sky conditions. Scene-dependent errors might be traceable to this assumption and modeling improvements would be necessary to eliminate such errors.

b. Intersatellite Calibration

The inter-satellite bias adjustments are determined with the collocated observations during the overlapping period for two satellites. Since the majority of collocations occur in the polar regions that the derived biases may not be representative for other climate zones. The revised OLR regression models v2.7 have significantly improved the consistency between OLR retrieved from different versions of HIRS instruments, thus reduced the range of the intersatellite adjustments by an order of magnitude, from 5 Wm^{-2} for the earlier v2.2 OLR models and decreased to 0.5 Wm^{-2} . Nevertheless, the possibility of scene-dependent inter-satellite biases still exists that becomes a possible source of errors for stability and trend.

6.1 Algorithm Performance

a. Geostationary observations

The availability of geostationary observations is not uniform over time. The complete coverage was not achieved until late 1998, due to the unavailability of the Indian geostationary data. It is in general very heterogeneous in terms of observing instruments and spatial coverage. This imposes risks of introducing artifacts to the daily OLR derivation. The blending procedure using “7-day boxcar” has put this into consideration, expecting that the grid-based calibration procedure can reliably remove the instrument and scene-dependent biases.

The quality of geostationary data is a major issue and is a very difficult problem. Bad data can be found that are probably caused by transmission interference, poor observations, or erroneous calibration processing, etc. It is a rather difficult task to identify and remove such bad data with an automated scheme. The quality of the Daily OLR CDR is clearly affected by the bad geostationary data and the issue has to be resolved.

b. HIRS observations

The temporal integral scheme can handle small amount of missing in the HIRS observations, e.g., typically the tropical orbital gaps. This scheme also enables the accurate derivation of daily OLR once there are sufficient data for Imager to HIRS calibration and the presence of Imager data in the target day. Extended missing of HIRS data, nevertheless, can cause lead to erroneous results and requires QC and manual removal.

For the days that daily OLR cannot be derived due to extended missing of HIRS observations, AVHRR observations can be used to fill the missing. The AVHRR OLR also

needs to be calibrated to the HIRS OLR on the grid-by-grid basis and over a short range of period before it can be used as a surrogate to HIRS OLR observations.

6.2 Sensor Performance

a. Radiometric Calibration

The Daily OLR CDR production performs radiance calibration following McMillin method. A set of coefficients is used in predicting calibration coefficients. This is to introduce instrument temperature dependence for the interpolation of the calibration coefficients between two calibration cycles. Neither the McMillin calibration method nor the operational version 4 calibration method handled the nonlinear responses. Accuracy of radiance can be improved if nonlinear response were accounted for.

b. Radiometric Noise

The Daily OLR CDR production package examines the quality flags of the HIRS level-1b data to determine if OLR retrieval can be performed. However, the OLR retrieval will still be performed when the sensor radiometric noise is higher than the instrument specification but the quality flag is not turned on. The recent HIRS instruments since NOAA-15 have shown sporadic problems that require ad hoc QC procedure to avoid contamination by the poor quality HIRS observations.

c. Spectral Response Function

The spectral response function has a role in the radiance calibration and in the radiance simulation. The accuracy of OLR estimation depends on the radiative transfer model simulations of the OLR flux and the HIRS radiances. Errors will be introduced if the pre-launch response function characterization is incorrect or the response functions have changed post-launch.

d. Instrument Scanning Alignment

There are known errors in the HIRS scanning operation on NOAA15 and 16. It is believed that the scanning is off by one scanning step position, in both satellites. Correction in the navigation parameters has already been applied in the level-1b data. Users should be aware of this error and use these data more cautiously.

7. Future Enhancements

The future enhancements are described in this section, in their priorities. Science Maintenance section laid out in the Production System Flow Chart (see **Figure 2**) also provides guidance for the possible areas of improvements.

7.1 Enhancement 1 – Missing Daily Fields

There are 205 days that are missing for Daily OLR v01r02 CDR due to HIRS instrument malfunctions or other reasons. The AVHRR observations could be used to provide surrogate OLR estimates, although with increased uncertainties. AVHRR OLR regression model needs to be redesigned to generate OLR estimate as consistent with HIRS as possible. The AVHRR OLR, similar to the Imager OLR, needs to be calibrated against HIRS OLR to maintain the same absolute radiometric reference. This will be done with the overlapping data in the days encompassing the missing days.

7.2 Enhancement 2 – Gridsat Quality Control

There are scan lines or regions that the Gridsat CDR data are considered bad data. It is very challenging to design algorithms and processes to identify and remove these data points. The effects of the bad Imager data can be seen in the v01r02 release of Daily OLR CDR as all the Gridsat data has entered the production flow with most bad data being passing through the simple threshold QC. Vigorous and robust QC needs to be devised and put in place either during the production of the Gridsat CDR or in the data ingestion stream during OLR CDR production.

7.3 Enhancement 3 – Temporal Integral Scheme

The “7-day boxcar” blending scheme serves two functions: a) calibration of Imager OLR against HIRS OLR; b) temporal integral. Depending on the availability of HIRS and Imager OLR data in the target day, the immediate neighboring days, and the entire boxcar, there are different paths to handle various situations. It is possible to improve the robustness and effectiveness of the classification of the scenarios and the branching for processing paths. The numerical integral using trapezoidal integral for determining the daily mean can also be improved. The Imager to HIRS calibration is performed on the running 7-day boxcar, thus certain degrees of smoothness and continuity is provided. The history and tracking of the calibration is useful to for such examination. Keeping the most recent calibration coefficients can provide a fallback solution when new calibration cannot be performed.

7.4 Enhancement 4 – Hyperspectral OLR Algorithms

Hyperspectral sounding instruments, including the AIRS, IASI and CrIS, are the new generation sounders. The development of OLR algorithms for these hyperspectral instruments (e.g., Lee et al., 2010), particularly the IASI and CrIS, are necessary for prolonging the OLR CDR beyond the HIRS era. Consistency of OLR estimated from the

hyperspectral and HIRS instruments are important so that the time series stability can be well maintained.

8. References

- Ba, M., R. G. Ellingson and A. Gruber, 2003: Validation of a technique for estimating OLR with the GOES sounder. *J. Atmos. Ocean. Tech.*, **20**, 79-89.
- Cressman, G. P., 1959: An operational objective analysis system. *Mon. Wea. Rev.*, **87**, 367-374.
- Ellingson, R. G. and M. Ba, 2003: A study of diurnal variation of OLR from the GOES Sounder. *J. Atmos. Ocean. Tech.*, **20**, 90-98.
- Ellingson, R. G., D. J. Yanuk, H.-T. Lee and A. Gruber, 1989: A technique for estimating outgoing longwave radiation from HIRS radiance observations. *J. Atmos. Ocean. Tech.*, **6**, 706-711.
- Ellingson, R. G., H.-T. Lee, D. Yanuk and A. Gruber, 1994: Validation of a technique for estimating outgoing longwave radiation from HIRS radiance observations, *J. Atmos. Ocean. Tech.*, **11**, 357-365.
- Knapp, K. R., S. Ansari, C. L. Bain, M. A. Bourassa, M. J. Dickinson, C. Funk, C. N. Helms, C. C. Hennon, C. Holmes, G. J. Huffman, J. P. Kossin, H.-T. Lee, A. Loew, G. Magnusdottir, 2011: Globally gridded satellite (GriSat) observations for climate studies. *Bulletin of American Meteorology Society*, 893-907. (doi: 10.1175/2011BAMS3039.1)
- Lee, H.-T., A. Heidinger, A. Gruber and R. G. Ellingson, 2004: The HIRS Outgoing Longwave Radiation product from hybrid polar and geosynchronous satellite observations. *Advances in Space Research*, **33**, 1120-1124.
- Lee, H.-T., R. G. Ellingson, and A. Gruber, 2010: Development of IASI outgoing longwave radiation algorithm. *Proceedings of the 2nd IASI International Conference*, Annecy, France, January 25-29, 2010.
- Lee, H.-T., R. G. Ellingson, and A. Gruber, 2010: Development of IASI outgoing longwave radiation algorithm. *Proceedings of the 2nd IASI International Conference*, Annecy, France, January 25-29, 2010.
- Lee, H.-T., 2014b: Daily OLR Climate Data Record – A challenge to homogenize operational satellite observations for climate applications. EGU General Assembly 2014, 27 April – 2 May, 2014, Vienna, Austria
- Lee, H.-T., C. J. Schreck, K. R. Knapp, 2014c: Generation of the Daily OLR Climate Data Record. 2014 EUMETSAT Meteorological Satellite Conference, 22-26 September 2014, Geneva, Switzerland
- GCOS: <http://www.wmo.int/pages/prog/gcos/index.php?name=EssentialClimateVariables> (as of July 19, 2011)
- NOAA Polar Orbiter Data (POD) User's Guide: 1998 version available online at <http://www.ncdc.noaa.gov/oa/pod-guide/ncdc/docs/intro.htm> as of July 18, 2011.
- NOAA KLM User's Guide: Feb. 2009 version available online at <http://www.ncdc.noaa.gov/oa/pod-guide/ncdc/docs/intro.htm> as of July 18, 2011.

Ohring, G., A. Gruber and R. G. Ellingson, 1984: Satellite determinations of the relationship between total longwave radiation flux and infrared window radiance. *J. climate & Appl. Meteor.*, **23**, 416-425.

Warner, J. X. and R. G. Ellingson, 2000: A new narrowband radiation model for water vapor absorption. *J. Atmos. Sci.*, **57**, 1481-1496.

Appendix A. Acronyms and Abbreviations

Acronym or Abbreviation	Meaning
AIRS	Atmospheric Infrared Sounder
AVHRR	Advanced Very High Resolution Radiometer
CATBD	Climate Algorithm Theoretical Basis Document
CDR	Climate Data Record
CERES	The Cloud and the Earth's Radiant Energy System
CrIS	Cross-track Infrared Sounder
ECT	Equator Crossing Time
EOS	Earth Observing System
ERBE	Earth Radiation Budget Experiment
ERBS	Earth Radiation Budget Satellite
EUMETSAT	European Organization for the Exploitation of Meteorological Satellites
FOV	Field of View
GCOS	Global Climate Observing System
GEO	Geosynchronous orbit
GERB	Geostationary Earth Radiation Budget Experiment
GOES	Geostationary Operational Environment Satellite
GridSat	Gridded Satellite (GridSat) - Geostationary
GSIP	GOES Surface and Insolation Product
IASI	Infrared Atmospheric Sounding Interferometer
HIRS	High-resolution Infrared Radiation Sounder
LEO	Low Earth Orbit
LUT	Lookup Table
LZA	Local Zenith Angle
MetOp	Meteorological Operational Polar Satellite
NASA	National Aeronautics and Space Administration
NESDIS	National Environmental Satellite, Data, and Information Service
NCDC	National Climatic Data Center
NOAA	National Oceanic and Atmospheres Administration
POES	Polar-orbiting Operational Environmental Satellite
TIROS	Television Infrared Observation Satellite

TOA	Top of Atmosphere
TOVS	TIROS Operational Vertical Sounder
WMO	World Meteorological Organization

Appendix B. Gridsat OLR Retrieval Algorithm

GridSat CDR data set provides inter-satellite calibrated and limb corrected brightness temperatures from geostationary satellite imaging instruments. Their time and spatial coverage of the available satellites is shown in **Figure B1**.

The instrument configurations on the geostationary satellites are not identical. While all of them have the 11 μm window channel, only the later ones have the 6.7 μm water vapor channel. The water vapor information is crucial for the accuracy in OLR estimation. The instantaneous OLR retrieval errors using only window channel is about 10 Wm^{-2} , while the errors can be halved to about 5 Wm^{-2} with the additional water vapor information. Two OLR models were developed and will be applied to the Imagers according to the availability of their radiance observations.

The OLR is determined with the flux equivalent temperature, T_f

$$OLR = \sigma T_f^4 \quad (\text{B1})$$

where σ is the Stefan-Boltzmann constant.

The One-channel OLR model is a quadratic form in the window channel brightness temperature, T_{win} :

$$T_f = T_{win}(c_{10} + c_{11}T_{win}) \quad (\text{B2})$$

The Two-channel OLR model is a quadratic form with the brightness temperatures of window and water vapor channels, T_{win} and T_{wv} :

$$T_f = T_{win}(c_{20} + c_{21}T_{win}) + T_{wv}(c_{22} + c_{23}T_{wv}) \quad (\text{B3})$$

The inter-satellite calibration of GridSat data is referenced to HIRS on NOAA-14 (Lei Shi and Ken Knapp, personal communications). Therefore the OLR models were developed with the NOAA-14 HIRS channels 8 and 12 nadir radiances.

The Imager OLR model v3 is determined with the same radiation simulation dataset as for the v2.2 HIRS OLR models.

Table 7 Coefficients for the One-Channel OLR model.

Terms	Coefficients	Uncertainty
C_{10}	1.24522	0.00397
C_{11}	-0.00117847	0.00001405

RMS error=10.3 Wm^{-2}

Table 8 Coefficients for the Two-Channel OLR model.

Terms	Coefficients	Uncertainty
C ₂₀	0	0
C ₂₁	8.58339e-4	4.72000e-6
C ₂₂	1.06098	5.45010e-3
C ₂₃	-1.12667e-3	2.43300e-5

RMS error=5.9 Wm⁻²

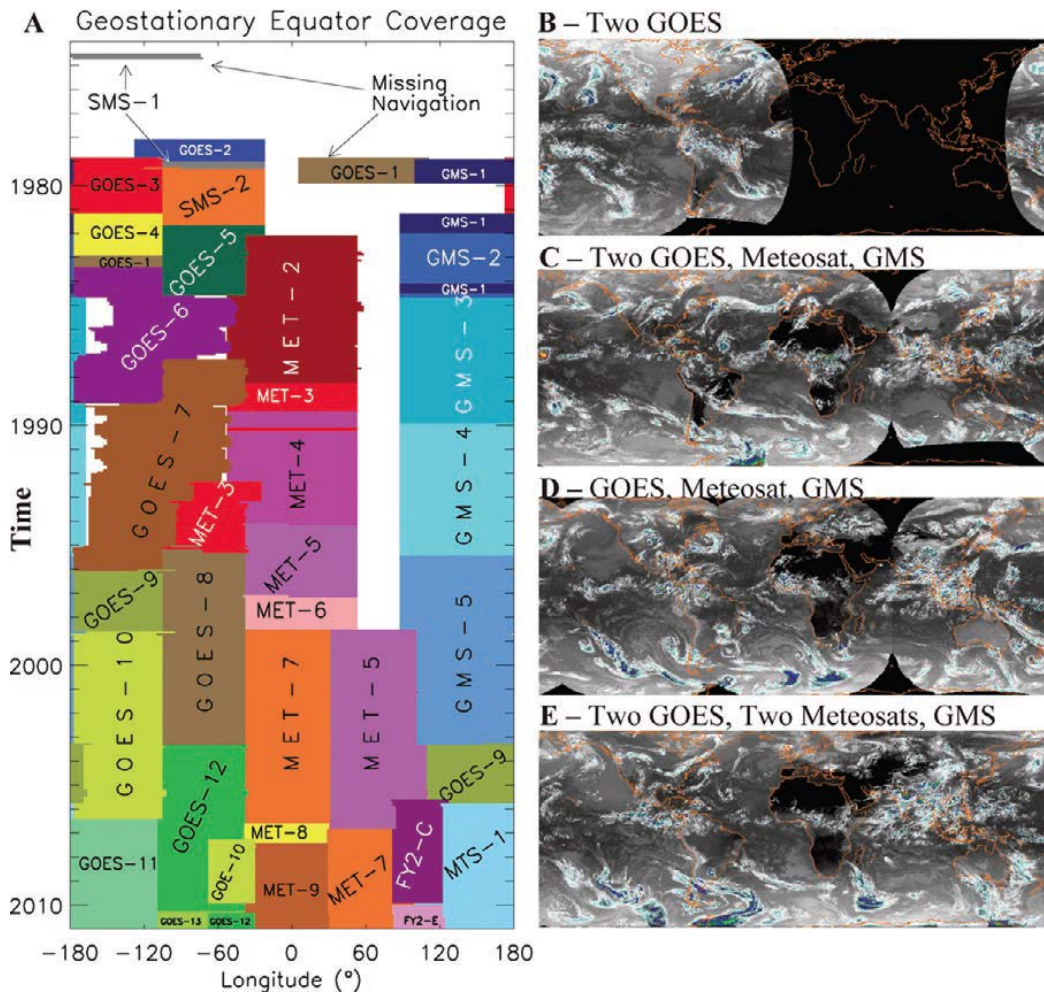


Figure B1 (a) Time series of ISCCP B1 geostationary satellite coverage at the equator (limited to a view zenith angle of 60° for illustrative purposes). (b)–(e) Sample GridSat coverage for typical satellite coverage: (b) two-satellite coverage with only GOES-East and -West in 1980, (c) four-satellite coverage that is typical of most of the period 1982–98, (d) typical three-satellite coverage when the United States was operating only one satellite (e.g., 1985–87 or 1989–92), and (e) five-satellite coverage that is typical of the current era (1998–present). (Figure copied from Knapp et al., 2011)

Appendix C. GSIP OLR Retrieval Algorithm

The Geostationary Surface Insolation Product (GSIP) is a NESDIS operational product. This product also generates OLR data from the geostationary Imagers observations.

The GSIP OLR algorithm v5 include OLR regression models for the Imagers on board GOES-8-15, MTSAT-1R/2, Meteosat-7 (MFG), and Meteosat 8-10 (MSG). The spectral response functions of these instruments are shown in **Figure C1**.

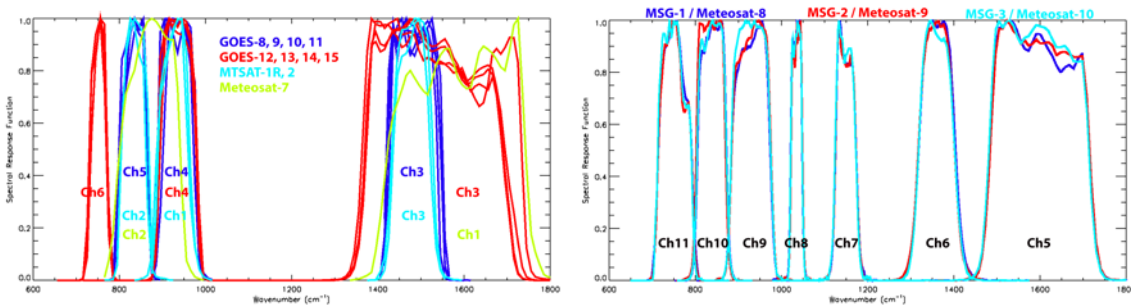


Figure C1 Spectral response functions for Imagers on board (a) GOES-8 to 15, MTSAT-1R/2 and Meteosat 7, and (b) Meteosat 8-10 satellites.

The OLR models for the respective instruments are described below.

GOES-8, 9, 10, and 11 Imagers:

$$OLR = a_0(\theta) + a_1(\theta)N_3^{0.5} + a_2(\theta)N_5 + a_3(\theta)N_5^2 \quad (C1)$$

GOES-12, 13, 14, and 15 Imagers:

$$OLR = a_0(\theta) + a_1(\theta)N_3^{0.2} + a_2(\theta)N_4 + a_3(\theta)N_6^{0.5} + a_4(\theta)N_6^2 \quad (C2)$$

MTSAT-1R and 2 Imagers:

$$OLR = a_0(\theta) + a_1(\theta)N_3^{0.5} + a_2(\theta)N_2 + a_3(\theta)N_2^2 \quad (C3)$$

Meteosat-7 (MFG) Imagers:

$$OLR = a_0(\theta) + a_1(\theta)N_1^{0.5} + a_2(\theta)N_2 \quad (C4)$$

Meteosat-8, 9 and 10 (MSG) Imagers, (SEVIRI):

$$OLR = a_0(\theta) + a_1(\theta)N_5^{0.5} + a_2(\theta)R_9 + a_3(\theta)R_{11}^{0.5} + a_4(\theta)R_{11}^2 + a_5(\theta)R_6^{0.2} \quad (C5)$$

The OLR regression coefficients for GSIP v5 algorithm are determined with the m2s3 radiation simulation of 3713 cases, with 4 outlier cases removed.